The Journal of Antibiotics (2018) 71:432–437
https://doi.org/10.1038/s41429-017-0015-x

JARA Japan Antibiotics Research Association
The Society for Actinomycetes Japan

ARTICLE

Two new secondary metabolites from a fungus of the genus *Robillarda*

Takeo Shimoyama[1] · Mizuki Miyoshi[1] · Tatsuo Nehira[2] · Atsuko Motojima[3] · Tsutomu Oikawa[3] · Olivier Laurence[4] · Yasuhiro Igarashi[1]

Received: 6 July 2017 / Revised: 8 November 2017 / Accepted: 17 November 2017 / Published online: 5 February 2018

Abstract

Two new compounds, robillafuran and (+)-robillapyrone, were isolated from the culture extract of a fungal strain of *Robillarda* along with (+)-monascuspyrone. The absolute configuration of (+)-robillapyrone and (+)-monascuspyrone was determined by ECD calculation. These three compounds showed preadipocyte differentiation activity at 10–40 μM.

Introduction

In fungal species, *Penicillium* and *Aspergillus* are the leading producers of secondary metabolites, accounting for more than 2000 known fungal bioactive compounds [1, 2]. The phylum Ascomycota to which these species belong contains a number of potential producers such as *Pestalotiopsis* and *Xylaria* [3, 4]. More specifically, these genera are classified under the order Xylariales. Species of this order are taxonomically diverse but many of them are not known or not evaluated as secondary metabolite producers. The genus *Robillarda* is one of such unexplored fungi. Species of *Robillarda* are found from live plants and decayed plant materials and also in soil and 38 species are listed [5]. However, there was no report on secondary metabolites from this genus to date. In our continuing investigation of chemical diversity in unexplored/underexplored microbes [6–8], a strain of *Robillarda* was found to produce new compounds robillafuran (**1**) and (+)-robillapyrone (**2**) along with (+)-monascuspyrone [9] (**3**) (Fig. 1). We herein describe the isolation and characterization of these compounds and their biological activity.

Results and discussion

Robillarda sp. MS9788 was cultured on A3M soft-agar medium that gave the most stable and the highest production results. This strain did not grow well in liquid medium or secondary metabolite production was not stable in solid medium composed of grains such as buckwheat and millet. HPLC-UV analysis of the culture extract indicated the presence of two major peaks displaying the UV spectra with the absorption maxima around 300 nm. Some minor peaks, one of which showed a UV spectrum similar to the major peaks, were also detected at earlier retention times. Several steps of chromatographic purification led to the isolation of one pyran (**1**) and two α-pyrone derivatives (**2** and **3**).

Robillafuran (**1**) was obtained as a pale yellow amorphous that gave an $[M+Na]^+$ peak at *m/z* 203.0678 in the positive-ion mode HR-ESITOFMS appropriate for a molecular formula of $C_{10}H_{12}O_3$ (Δ −0.1 mmu, calcd. for $C_{10}H_{12}O_3Na$ 203.0679). The IR spectrum displayed the absorption band at 1702 cm^{-1} for the ester carbonyl group. ^{13}C NMR and HSQC spectral data established 10 carbons

This article is dedicated to Prof. Hamao Umezawa on the occasion of the 60th anniversary of worldwide marketing of kanamycin.

Electronic supplementary material The online version of this article (https://doi.org/10.1038/s41429-017-0015-x) contains supplementary material, which is available to authorized users.

✉ Yasuhiro Igarashi
yas@pu-toyama.ac.jp

[1] Biotechnology Research Center and Department of Biotechnology, Toyama Prefectural University, 5180 Kurokawa, Imizu, Toyama 939-0398, Japan

[2] Graduate School of Integrated Arts and Sciences, Hiroshima University, 1-7−1 Kagamiyama, Higashi-Hiroshima 739−8521, Japan

[3] School of Nutrition and Dietetics, Kanagawa University of Human Services, 1-10-1 Heisei-cho, Yokosuka, Kanagawa 238-8566, Japan

[4] Mycosphere, 20, Avenue Jean Jaurès, 47500 Fumel, France

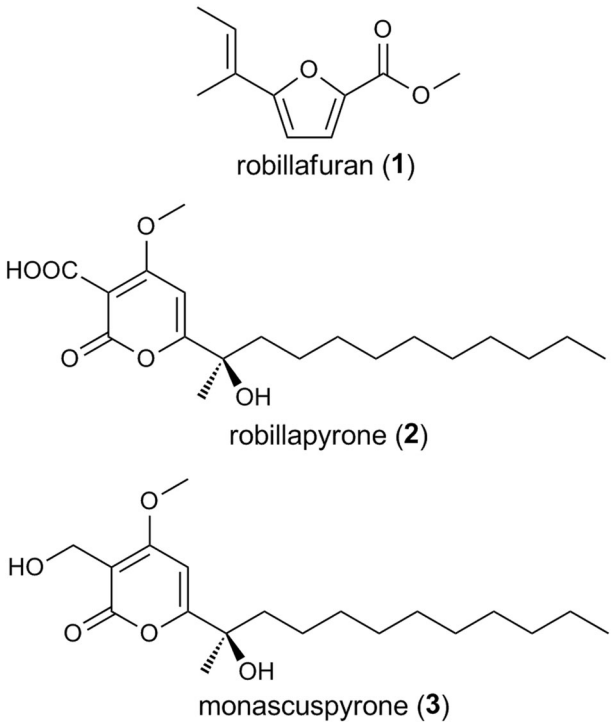

Fig. 1 Structures of robillafuran (**1**), (+)-robillapyrone (**2**), and (+)-monascuspyrone (**3**)

Table 1 ^{1}H and ^{13}C NMR data for robillapyran (**1**) in CD_3OD

Position	δ_H mult (*J* in Hz)[a]	δ_C[b]	HMBC[c]
1	1.88 d (7.15)	14.4	3
2	6.65 q (7.15)	131.2	4, 9
3		128.5	
4		162.9	
5	6.14 d (2.05)	99.0	3, 4
6	5.59 d (2.05)	88.8	7, 8
7		167.2	
8		174.3	
9	1.90 s	12.3	2, 3, 4
10	3.88 s	57.2	8

[a] Recorded at 500 MHz

[b] Recorded at 125 MHz

[c] HMBC correlations are from proton(s) stated to the indicated carbon

that were assigned to two methyls, one methoxy, three olefinic methines, one quaternary sp^2 carbon, and three oxygenated sp^2 carbons (Table 1). COSY spectrum showed correlations between the methyl and an olefinic proton (H1/H2) and between olefinic protons (H5/H6) (Fig. 2). The doublet methyl H1 showed HMBC correlations to two olefinic carbons C2 and C3, and the singlet methyl H9 showed correlations to three sp^2 carbons C2, C3, and C4. These correlation data established 1-methyl-1-propenyl group connecting at C4. Protons H5 and H6 were HMBC-correlated to C3 and C4, and C7 and C8, respectively, which confirmed the carbon connectivity from C3 to C8. The methoxycarbonyl group at C7 was confirmed by an HMBC correlation from the methoxy protons H10 to the carbonyl carbon C8. Finally, the oxygen atom was placed between C4 and C7 in consideration of the chemical shifts of these carbons as well as the molecular formula. The *E* configuration of the double bond between C2 and C3 was deduced on the basis of NOESY analysis in which correlations were not detected for H2/H9 or H1/H5 while the correlation was observed between H5 and H9.

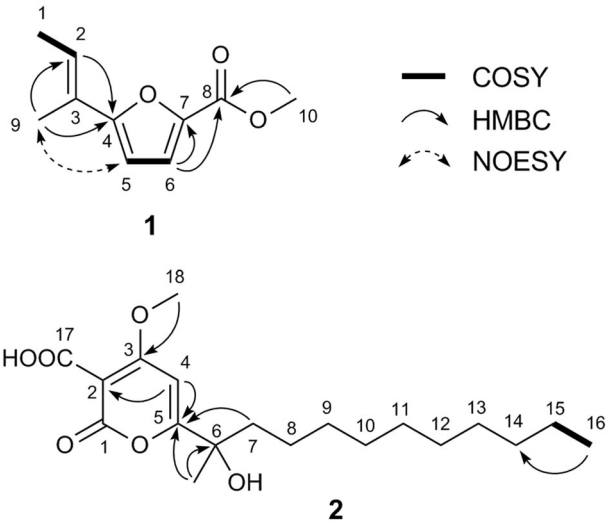

Fig. 2 Selected 2D NMR correlations for **1** and **2**

Robillapyrone (**2**) was obtained as a colorless oil. The molecular formula of $C_{19}H_{30}O_6$, established by the HR-ESITOFMS data (*m/z* 377.1940 for $[M+Na]^+$, Δ −0.1 mmu, indicating two hydrogen loss and one oxygen addition compared to monascuspyrone (**3**). The UV spectrum showed an absorption band at 304 nm, slightly red-shifted comparing with **3** that showed λ_{max} at 298 nm. Analysis of the ^{1}H and ^{13}C spectra revealed the presence of one triplet and one singlet methyls, one methoxy group, nine methylenes, one olefinic methine, and six quaternary carbons (one oxygenated sp^3, one non-oxygenated and four oxygenated sp^2). Six sp^2 carbons and the methoxy group could be assigned to constitute the α-pyrone moiety in comparison with the NMR data of **3** and by analysis of HMBC correlation data. The only significant difference of NMR data between **2** and **3** was the presence of an additional oxygenated sp^2 carbon and the absence of the oxygenated methylene in **2**. There are four oxygenated sp^2 carbons (δ_C: 162.1, 167.6, 175.1, and 176.1) in **2**, whereas three (δ_C: 164.9, 167.0, and 170.6) in **3**, suggestive of the replacement of the hydroxymethyl group of **3** with a carboxyl group. This was supported by the IR spectrum of **3** that displayed an absorption band at 1729 cm^{-1} for the carboxylic acid. HMBC correlations from H18 to C3 and H4 to C2 and C5

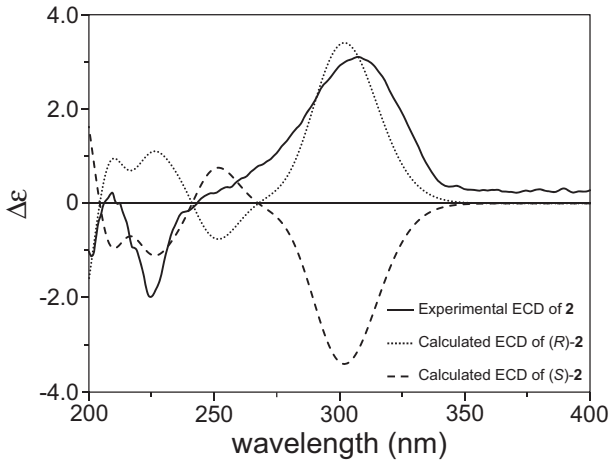

Fig. 3 Calculated and experimental ECD spectra of (+)-**2**

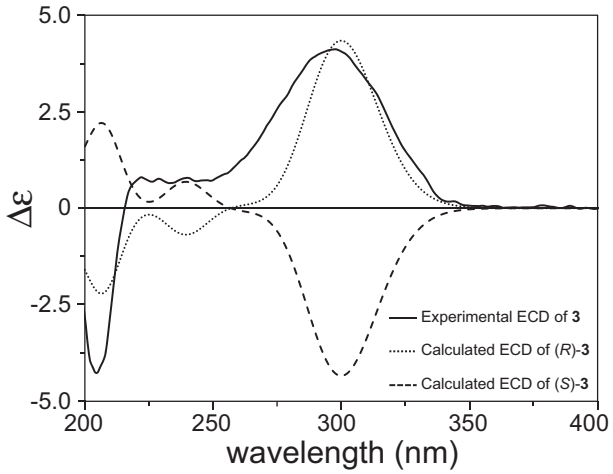

Fig. 4 Calculated and experimental ECD spectra of (+)-**3**

established the connectivity of the carbons from C2 to C5. The remaining two carbons at δ_C 162.1 and 167.6 were assigned to the pyrone carbonyl carbon C1 and the carboxyl carbon C17 connecting at C2. The 11-carbon alkyl chain bearing a tertiary hydroxy group and a methyl group (C19) was connected to C5 on the basis of the HMBC correlations from H7 and H19 to C5 to complete the planar structure of **2** (Fig. 2).

Monascuspyrone (**3**) was first reported from *Monascus pilosus* without stereochemical assignment, but its specific rotation was zero, implying that it was a racemate [9]. Meanwhile, monascuspyrone (**3**) produced by *Robillard* sp. MS9788 was chiral with the positive specific rotation ($[\alpha]_D$ + 53). Robillapyrone (**2**) also showed the same positive sign and the similar absolute value of specific rotation ($[\alpha]_D$ + 31), suggestive of the same absolute configuration for these compounds. In the electronic circular dichroism (ECD) spectra, both (+)-**2** and (+)-**3** displayed a negative and a positive Cotton effects around 210 and 300 nm, respectively. As no empirical rule was applicable to the compounds, we performed theoretical calculations [10–12] to predict the experimental ECD spectra of (+)-**2** and (+)-**3**. A thorough evaluation of stable conformers was carried out, since both (+)-**2** and (+)-**3** have the same flexible 11-carbon chain that inevitably raises the number of stable conformers. Under a systematic alteration of the eleven-carbon chain of (+)-**2** and (+)-**3**, conformational searches with molecular mechanics [13–15] and subsequent structure optimizations with quantum mechanics [16] were performed. Relevant stable conformers were subjected to the ECD calculations with quantum mechanics [16] at high approximation. As a result, it was shown that all evaluated conformers had the positive Cotton effect at 290–300 nm, whereas the sign of the Cotton effect at 210 nm varied between conformers. Consequently, the absolute configurations of (+)-**2** and (+)-**3** were represented dominantly with the positive Cotton effect at 290–300 nm. The calculated ECD spectrum of the *R*-enantiomer of (+)-**2** showed a good accordance with the experimental ECD spectrum (Fig. 3). The calculated ECD of (*R*)-(+)-**3** was also in good agreement with the experimental data of (+)-**3** (Fig. 4). Therefore, the absolute configuration at C6 of (+)-**2** and (+)-**3** was determined to be *R*.

Adipocyte differentiation is the process of cell differentiation in which preadipocytes change into adipocytes [17]. The key function of mature adipocytes is the secretion of adiponectin, which enhances glucose uptake and improves insulin sensitivity in type 2 diabetes patients [18]. Therefore, inducers of preadipocyte differentiation can be a promising therapeutic agent for insulin resistance and type 2 diabetes [19]. Inducing potential of robillafuran (**1**), (+)-robillapyrone (**2**), and (+)-monascuspyrone (**3**) for murine ST-13 preadipocyte differentiation were evaluated at concentrations of 10–40 μM by analyzing the accumulation of lipid droplets [20]. **1** was weakly active (50% differentiation) at 40 μM, while (+)-**2** induced *ca*. 90% differentiation at 40 μM. Both **1** and (+)-**2** displayed no toxic or growth-retarding effect on ST-13 cells at 40 μM. (+)-**3** was the most potent among the three compounds: 80–100% of preadipocytes were differentiated at 10–20 μM (Fig. 5). At 40 μM, (+)-**3** inhibited the growth of preadipocyte cells although it was not toxic.

In conclusion, our chemical investigation of *Robillarda* sp. MS9788 resulted in the isolation of two new compounds robillafuran (**1**) and (+)-robillapyrone (**2**). This is the first report on the secondary metabolites from the genus *Robillarda*. This finding supports the idea that consideration of taxonomic position is essential to the discovery of new chemical entities. Continuous screening efforts along this line will further disclose the biosynthetic potential of unexplored species.

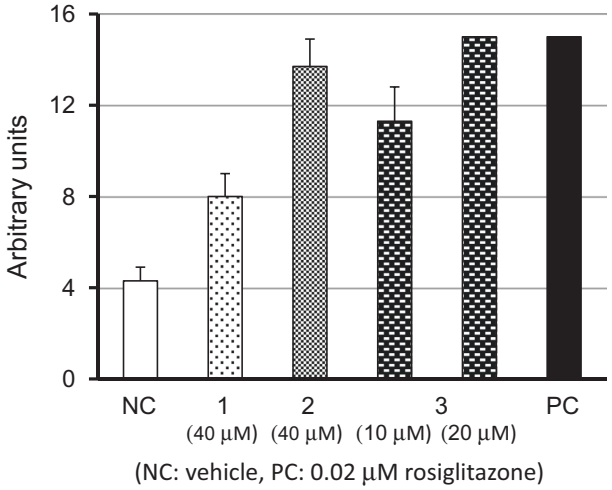

Fig. 5 Induction of adipocyte differentiation by **1–3**

Experimental section

General experimental procedures

UV spectra were recorded on a Hitachi U-3210 spectrophotometer, and IR spectra on a Perkin-Elmer Spectrum 100. Optical rotations were measured using a JASCO DIP-3000 polarimeter, and CD spectra on a JASCO J-720W spectropolarimeter. NMR spectra were obtained on a Bruker AVANCE 500 spectrometer in $CDCl_3$ using the signals of the residual solvent protons (δ_H 7.26) and carbons (δ_C 77.0) as an internal standard. HR-ESITOFMS were recorded on a Bruker microTOF focus.

Fungal strain

The producing strain MS9788 was isolated from submerged decaying stems of *Phragmipes* sp. by Olivier Laurence (Mycosphere, France) during a fungal survey expedition near the Kaw swamps (French Guyana) in 2009. The strain was identified as *Robillarda* based on the gene sequence of the D1/D2 domain of 28S rRNA gene. Strain MS9788 (562 nucleotides, DDBJ accession number LC309276) showed 98.3% similarity to *Robillarda sessilis* BCC13393 (accession number FJ825378) and *Robillarda sessilis* CBS 114312 (accession number KR873284).

Fermentation

A piece of MYA2 agar medium [2.0% malt extract (Difco Laboratories), 0.1% yeast extract (Kyokuto Chemical Co., Japan), and 1.5% agar] on which *Robillarda* sp. MS9788 was growing was inoculated onto twenty 500-mL K-1 flasks each containing 100 mL of A3M soft-agar medium [0.5% glucose, 2.0% glycerol, 2.0% soluble starch, 1.5% Pharmamedia (Trader's protein), 0.3% yeast extract, and 0.4% agar]. The flasks were placed in dark at 25 °C for 30 days without shaking. An aliquot of 100 mL of 1-butanol was added to each flask and the flasks were agitated for 1 h on a rotary shaker at 30 °C. The organic layer was separated by centrifugation (4000 rpm, 10 min) and concentrated to give crude extract (37.4 g).

Isolation

A portion (5.25 g) of the crude extract was subjected to silica gel column chromatography with a step gradient of $CHCl_3$/MeOH (1:0, 20:1, 10:1, 4:1, 2:1, 1:1, and 0:1 v/v). The fraction eluted with 4:1 $CHCl_3$–MeOH was containing the target peaks and concentrated to give 817 mg of brown oil, which was further purified by reversed phase ODS column chromatography with a gradient of MeCN/0.1% HCO_2H (2:8, 3:7, 4:6, 5:5, 6:4, 7:3, and 8:2 v/v). The 5:5 fraction (27 mg) was evaporated and the remaining aqueous solution was extracted with EtOAc, and the organic layer was concentrated to dryness. The residual amorphous solid was purified by reverse-phase HPLC using a Cosmosil 5C18-AR-II column (Nacalai Tesque Inc., 10 × 250 mm) with a linear gradient of MeCN/0.1% HCO_2H (40:60–50:50) over 30 min at a flow rate of 4 mL/min, followed by evaporation and extraction with EtOAc, yielding robillafuran (**1**, 8.6 mg, t_R 12.7 min). Similarly, the 7:3 ODS fraction (37 mg) was purified by preparative HPLC with isocratic elution (MeCN/0.1% HCO_2H = 52:48) to give (+)-monascuspyrone (**3**, 9.6 mg, t_R 22.8 min). HPLC purification of the 8:2 ODS fraction (38 mg) gave (+)-robillapyrone (**2**, 16.6 mg, t_R 26.6 min).

Robillafuran (**1**): Pale yellow amorphous; UV (MeOH) λ_{max} (log ε) 224 (4.77), 310 (4.29) nm; IR (ATR) ν_{max} 1702, 1076 cm^{-1}; ^1H and ^{13}C NMR data, see Table 1; HR-ESITOFMS $[M+Na]^+$ 203.0678 (calcd for $C_{10}H_{12}O_3Na$, 203.0679).

(+)-*Robillapyrone* (**2**): Colorless oil; $[\alpha]^{21}_D + 31$ (*c* 0.16, MeOH); UV (MeOH) λ_{max} (log ε) 207 (4.18), 304 (3.82) nm; CD (MeCN) $\Delta\varepsilon_{216} - 1.98$, $\Delta\varepsilon_{303} + 3.11$; IR (ATR) ν_{max} 3405, 1729, 1668, 1238 cm^{-1}; ^1H and ^{13}C NMR data, see Table 2; HR-ESITOFMS $[M+Na]^+$ 377.1940 (calcd for $C_{19}H_{30}O_6Na$, 377.1941).

(+)-*Monascuspyrone* (**3**): Colorless oil; $[\alpha]^{21}_D + 53$ (*c* 0.21, $CHCl_3$) {lit. $[\alpha]^{22}_D \pm 0$ (*c* 0.08, $CHCl_3$)}; UV (MeOH) λ_{max} (log ε) 206 (4.21), 298 (3.68) nm; CD (MeCN) $\Delta\varepsilon_{205} - 4.29$, $\Delta\varepsilon_{298} + 4.12$; IR (ATR) ν_{max} 3366, 1665, 1258 cm^{-1}; ^1H and ^{13}C NMR data, see Table 2; HR-ESITOFMS $[M+Na]^+$ 363.2148 (calcd for $C_{19}H_{32}O_5Na$, 363.2147).

Table 2 ^{1}H and ^{13}C NMR data for robillapyrone (**2**) and monascuspyrone (**3**) in $CDCl_3$

Position	Robillapyrone (**2**)			Monascuspyrone (**3**)	
	δ_H mult (J in Hz)[a]	δ_C[b]	HMBC[c]	δ_H mult (J in Hz)	δ_C[b]
1		167.6			164.9
2		94.6			103.8
3		176.1			167.0
4	6.81 s	94.3	2, 5, 6	6.52 s	92.2
5		175.1			170.6
6		74.6			74.1
7	1.76 ddd (13.8, 12.4, 4.6)	40.7	5, 6, 8, 19	1.71 ddd (13.9, 12.2, 4.5)	40.6
	1.93 ddd (13.8, 12.4, 4.6)			1.91 ddd (13.9, 12.2, 4.5)	
8	1.11 m	23.6		1.13 m	23.5
	1.40 m			1.34 m	
9	1.25–1.31 m	29.5[d]		1.11–1.39 m	29.3[e]
10	1.25–1.31 m	29.6[d]		1.11–1.39 m	29.47[e]
11	1.25–1.31 m	29.7[d]		1.11–1.39 m	29.54[e]
12	1.25–1.31 m	29.7[d]		1.11–1.39 m	29.54[e]
13	1.25–1.31 m	29.9[d]		1.11–1.39 m	29.6[e]
14	1.25 m	32.1		1.25 m	31.9
15	1.26 m	22.9	14, 15	1.25 m	22.7
16	0.88 t (6.8)	14.3		0.88 t (6.8)	14.1
17		162.1		4.56 s	54.7
18	4.18 s	58.7	3	3.95 s	56.6
19	1.58 s	27.5	5, 6, 7	1.52 s	27.3

[a] Recorded at 500 MHz

[b] Recorded at 125 MHz

[c] HMBC correlations are from proton(s) stated to the indicated carbon

[d,e] Interchangeable

ECD calculation

Theoretical electron circular dichroism (ECD) spectra were obtained by integrating a typical calculation procedure [10–12] and a strategic structure modification. Conformational searches were performed with CONFLEX7 (Ver. 7. A.0910 by CONFLEX, Tokyo) [13–15] using a commercially available PC (operating system: Windows7 Professional SP1 64-bit, CPU: QuadCore Xeon E3-1225 processor 3.10 GHz, RAM 8 GB) and density functional theory (DFT) calculations were conducted with Gaussian 09 (Revivion D.01 by Gaussian, Wallingford, CT) [16] with a PC (Operating System: CentOS 6.5 a Linux, CPU: 12 Intel Xeon E5-2643 v3 processors 3.40 GHz, RAM 32 GB).

The numbers of relevant conformers for **2** and **3** that possess a flexible 11-carbon alkyl chain were reduced based on a strategic modification of the alkyl chain. The 11-carbon alkyl chain of **2** was stepwise shortened to 7-carbon and expanded to 13-carbon. All the structures of interest were composed and subjected to conformational searches with CONFLEX7 using MMFF94S (2010-12-04HG) as the force field, where initial stable conformers were generated for up to 50 kcal/mol. In cases there were conformers with >1% of abundance (7-, 8-, and 9-carbon derivatives), all of those stable conformers were subjected to further structure DFT-based optimizations with B3LYP/6-31G(d) using acetonitrile as the solvent with the polarizable continuum model (PCM) method. In other cases (10-, 11-, 12-, and 13-carbon derivatives), over 100,000 stable conformers were found and no conformer showed >1% of abundance. Based on the results from the above-mentioned shorter-chained derivatives, conformers used for the further calculations were limited for only the most stable six conformers. The selected stable conformers were then relayed to the time-dependent density functional theory-based (TDDFT-based) ECD calculations with B3LYP/cc-pVDZ using acetonitrile as the solvent. As a result, all the considered stable conformers, whatever the chain lengths were, possessed the positive ECD peak at 290 nm, for which the wavelengths of the calculated UV spectra were corrected to reproduce the absorption at 300 nm. For the genuine **2** with the flexible 11-carbon alkyl chain, the outstandingly most stable four conformers were selected. The obtained rotational strengths were converted into Gaussian curves (bandwidth sigma = 3000 cm^{-1}). The resultant ECD spectra were summed based on the Bolzmann distribution to give the ECD spectrum.

The same calculation strategy was applied to **3**, except that the 11-carbon chain modification was considered with only 10-carbon and 12-carbon chain models. Derived was the same conclusion that the ECD signs at 290 nm for all conformers of the simulated models with the *R* configuration at C6 were positive.

Biological assay

Adipocyte differentiation assay was carried out according to the procedure previously described [21–23]. Rosiglitazone, an antidiabetic drug, was used as a positive control in the adipocyte differentiation assay. It induced differentiation in 80% of murine ST-13 preadipocyte cells at 0.02 μM.

Acknowledgements This research was supported by JSPS KAKENHI Grant No. JP16K07719 to YI and a Grant-in-Aid for Scientific Research (A) (25252037) from JSPS to TO.

Compliance with ethical standards

Conflict of interest The authors declare that they have no conflict of interests.

References

1. Bérdy J. Bioactive microbial metabolites. J Antibiot. 2005;58: 1–26.
2. John B. Dictionary of natural products on DVD, version 23:1. UK: The Chapman & Hall/CRC Press, Taylor & Francis Group; 2014.
3. Yang XL, Zhang JZ, Luo DQ. The taxonomy, biology and chemistry of the fungal *Pestalotiopsis* genus. Nat Prod Rep. 2012;29:622–41.
4. Song F, Wu SH, Zhai YZ, Wang T. Secondary metabolites from the genus *Xylaria* and their bioactivities. Chem Biodivers. 2014;11:673–94.
5. Royal Botanic Gardens, Kew and the Institute of Microbiology, Chinese Academy of Sciences. Index Fungorum. http://www.indexfungorum.org/names/Names.asp. Accessed 8 November 2017.
6. Fukuda T, Sudoh Y, Tsuchiya T, Okuda T, Igarashi Y. Isolation and biosynthesis of preussin B, a pyrrolidine alkaloid from *Simplicilium lanosoniveum*. J Nat Prod. 2014;77:813–7.
7. Akiyama H, et al. Metabolites from thermophilic bacteria I: *N*-Propionylanthranillic acid, a co-metabolite of the bacillamide class antibiotics and tryptophan metabolites with herbicidal activity from *Laceyella sacchari*. J Antibiot. 2014;67: 459–63.
8. Igarashi Y, et al. Avellanin C, an inhibitor of quorum-sensing signaling in *Staphylococcus aureus*, from *Hamigera ingelmeimensis*. J Antibiot. 2015;68:707–10.
9. Cheng M-J, Wu M-D, Chen I-S, Yang P-S, Yuan G-F. Secondary metabolites isolated from the fungus *Monascus pilosus*. Rev Roum Chim. 2010;55:335–41.
10. Bringmann G, Bruhn T, Maksimenka K, Hemberger Y. The assignment of absolute stereostructures through quantum chemical circular dichroism calculations. Eur J Org Chem. 2009;2009: 2717–27.
11. Matsumoto K, et al. Phenyl-(2-pyridyl)-(3-pyridyl)-(4-pyridyl) methane: synthesis, chiroptical properties, and theoretical calculation of its absolute configuration. Chem Asian J. 2007;2:1031–6.
12. Pescitelli G, Di Pietro S, Cardellicchio C, Capozzi MAM, Di Bari L. Systematic investigation of CD spectra of aryl benzyl sulfoxides interpreted by means of TDDFT calculations. J Org Chem. 2010;75:1143–54.
13. Goto H, Obata S, Nakayama N, Ohta K. CONFLEX 7. Tokyo, Japan: CONFLEX Corporation; 2012.
14. Goto H, Osawa E. Corner flapping: a simple and fast algorithm for exhaustive generation of ring conformations. J Am Chem Soc. 1989;111:8950–1.
15. Goto H, Osawa E. An efficient algorithm for searching low-energy conformers of cyclic and acyclic molecules. J Chem Soc Perkin Trans. 1993;2:187–98.
16. Frisch MJ et al. Gaussian 09, Revision D.01. Wallingford, CT, USA: Gaussian, Inc.; 2013.
17. Cornelius P, et al. Regulation of adipocyte development. Annu Rev Biochem. 1994;14:99–129.
18. Ukkola O, et al. Adiponectin: a link between excess adiposity and associated comorbidities? J Mol Med. 2002;80:696–702.
19. Kadowaki T, et al. Adiponectin and adiponectin receptors in insulin resistance, diabetes, and the metabolic syndrome. J Clin Invest. 2006;116:1784–92.
20. Kunimasa K, et al. Identification of nobiletin, a polymethoxyflavonoid, as an enhancer of an adiponectin secretion. Bioorg Med Chem Lett. 2009;19:2062–4.
21. Ikeda M, et al. Norlichexanthone isolated from fungus P16 promotes the secretion and expression of adiponectin cultured in ST-13 adipocytes. Med Chem. 2011;7:250–6.
22. Igarashi Y, et al. Prajiamide, a new modified peptide from a soil-derived *Streptomyces*. J Anitibiot. 2012;65:157–9.
23. Indananda C, Igarashi Y, Ikeda M, Oikawa T, Thamchaipenet A. Linfuranone A, a new polyketide from plant-derived *Microbispora* sp. GMKU 363. J Antibiot. 2013;66:675–7.